Journal of the Korean Nuclear Society
Volume 6, Number 4, December 1974

《Original》

Pulsed Ionization Chamber Technique for Measurement of Recombination Rate of Plasmas

Sang Hoon Kim

Department of Nuclear Engineering Han Yang University, Seoul, Korea

(Received July 22, 1974)

Abstract

The output signal voltage of the pulsed ionization chamber (PIC) was measured for a range of electron density (10^{13}-$10^{17}m^{-3}$) of the ^3He plasmas. This experimental data was in excellent agreement with the theory including space charge effects.

As an application of the PIC techniques, two-body recombination coefficients were obtained with electron densities measured from output signal voltage of the PIC. These values as a function of pressure were in good agreement with theoretical predictions and ranged from 5×10^{-14} to 3×10^{-13} (m^3/sec) at 300° K for 1 to 10 atmospheric ^3He plasma.

요 약

펄스된 이온화상자(PIC)의 출력 신호전압이 전자밀도가 10^{13}—$10^{17}m^{-3}$인 ^3He 플라즈마들에 대해 측정되었다.

이 PIC 기술의 한 응용으로서 이체 재결합 상수들이 PIC의 출력신호전압으로 측정된 전자밀도들로부터 구해졌다. 압력의 함수로서의 이 값들은 이론적인 예측과 잘 부합하며, 수치는 300°K에 있는 1-10기압의 ^3He 플라즈마에 대해 5×10^{-14}—3×10^{-13} m^3/sec의 범위에 있다.

1. Introduction

A recent application of the ionization chamber has been in the study of ionized gas kinetics in high radiation fields by the application of a pulsed high voltage collection potential instead of a constant high voltage. Since this pulsed ionization chamber (PIC) has shorter measuring times for measurements of electron densities ($\sim10^{-6}$ sec) compared with other diagnostic tools, for example, the Langmuir probe does ($>10^{-3}$ sec), it can be used exclusively for the plasma kinetic study such as the plasma growth and decay proce-

sses within the gas filled pipe in the nuclear reactor core.

The theory of the pulsed ionization chamber concerning space charge effects has been recently made by the authors of this paper for measurements of high electron densities ranging from 10^{10} to $10^{20}\,m^{-3}$ [1]. The following in this paper is the detailed description of electronic setups with ^3He filled ion chambers of coaxial geometry, operated in the PIC mode. With these setups, the pulse profiles are measured, and compared with the numerical results based on the above theory. As an application of this technique, the recombination rate of the helium is measured by measuring either the electron density at steady state or its time dependency during growth interval using the $^3H(np)t$ reaction for producing electron densities ranging 10^{13} to $10^{17}\,m^{-3}$ within the sensitive volume of the ionization chamber.

This paper should be read in conjunction of Ref. 1. The authors will follow the notation of Ref. 1, and equations given there will not be repeated here.

2. Experimental System of Pulsed Signal Measurements

The chamber having cylindrical coaxial electrode geometry is shown in Fig. 1 where guard rings establish the limits of the sensitive volume and minimize the effects of diffusion into and out of the sensitive volume. This chamber is placed in the radiation field.

The circuit shown schematically in Fig. 2 is a simplification of the one that is used for the pulsed high voltage mode of operation. In the figure C_1 is the capacitance of the ionization chamber, C_2 the stray capacitance associated with high voltage pulser coupling circuit and the collection output circuit, and R the net shunt resistance of the collection output circuit. The sequence of operation of such electronic system is shown in Fig. 3.

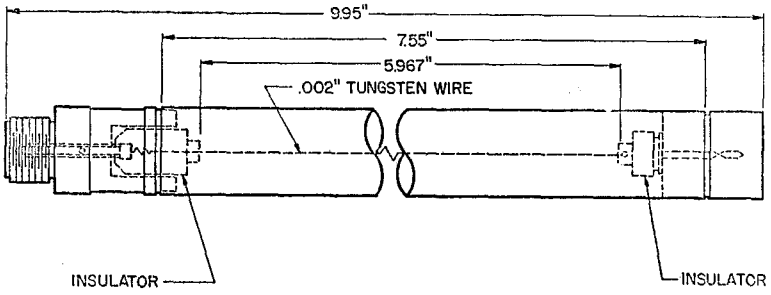

Fig. 1. Ionization chamber configuration.

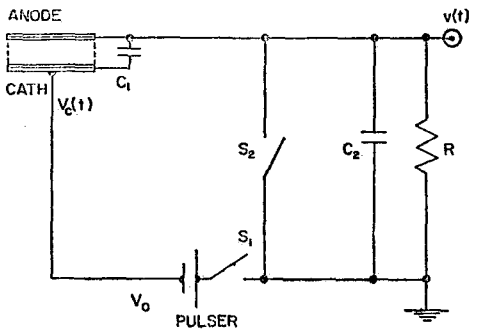

Fig. 2. Schematic diagram of equivalent circuit for pulsed ionization chamber circuit.

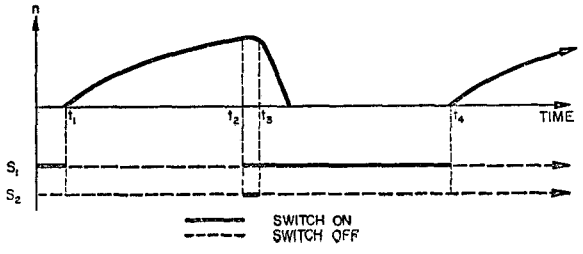

Fig. 3. Operation sequence of switches and time dependence of electron population.

Switches S_1 and S_2 in this figure represent a fast rise high voltage pulser and a fast switching biased diode, respectively.

During the sequence of on and off operations of switches S_1 and S_2, the charge and voltage configurations of the ionization chamber and its external *RC* circuit are in the following:

1) During the initial period from t_1 and t_2, the switches S_1 and S_2 are opened. The plasma is generated within the sensitive volume of ^{3}He filled ionization chamber, placed in the thermal column of the nuclear reactor. During the slow down of the charged products of an exoergic nuclear reaction $^3He+n\rightarrow{}^1H+{}^3H+764$ Kev. The Q of the reaction is partitioned between the two products as kinetic energy. Through the slowing down process, the kinetic energy is dissipated in the helium gas as ionization and excitation, producing on the average approximately 2 to 3×10^{14} ion pairs per interaction. This ionization is allowed to build up in the gas within the ionization chamber.

The time rate change of the plasma density N during growth can be represented by the equation

$$\frac{dN(t)}{dt}=S-\{\alpha_2-\alpha_3N(t)\}N^2(t)-\frac{D}{L^2}N(t)-kN(t) \quad (1)$$

where

S=source term

α_2=two body recombination coefficient

α_3=three body recombination coefficient

D=ambipolar diffusion coefficient

L=diffusion length

k=electron attachment coefficient.

The soure term S which represents the rate of ionization of the helium gas can be written as

$$S=\phi N_{He}\sigma\bar{E}/W \quad (2)$$

were

ϕ=termal neutron flux density

N_{He}=^{3}He atom density

σ=5400 barns, thermal neutron reaction cross section

W=average energy required to produce an ion pair

E=average energy deposited in the gas by the (n,p) reaction products.

2) During t_2 to t_3, the switches S_1 and S_2 are closed. The ionization chamber having the capacitance C_1 is rapidly charged by the

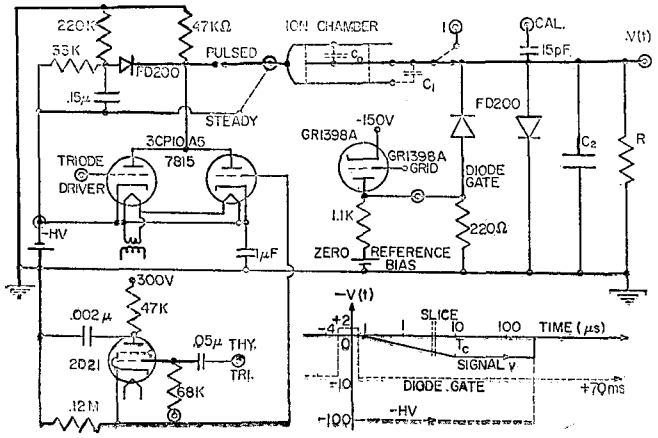

Fig. 4. Circuit of pulser and signal collection.

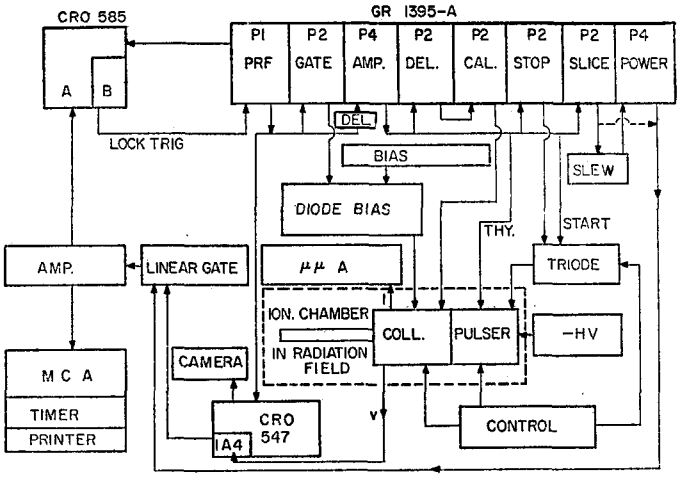

Fig. 5. Detailed blockdiagram of experimental appratus for measuring signal voltage and saturation current.

voltage supply pulser. This is accomplished through the application of a negative potential (−10V) to the grid of the GR-1398A triode (duration time of about 0.5 ms), switching the tube off as seen in Fig. 4 and 5, 0.4 ms prior to the application of high voltage supply pulse (about 200V/cm). The high voltage supply pulse has a rise time of about a nanosecond and is constant afterwards. The diode (FD 200) becomes conductive approximately 0.5 ms later due to the positive potential (2V) supplied by the off-set DC battery which supplies the zero reference bias (see Fig. 4). This forward-biasing of the diode causes the capacitance of the ionization chamber C_1 to be charged in the order of 0.5 ms due to the lowest impedance state of the external circuit (theoretically zero RC time constant). As this charging time is very short compared with that required for the total electron collection ($\bar{t}_c \simeq 10$mc), the former time interval (from t_2 to t_3) can be neglected with respect to the electron collection time. This allows that C_1 is initially charged ($q_0 = C_1 V_0$).

3) During t_4 to t_5, the switch S_2 is opened while the switch S_1 remains closed. This is accomplished by removing the negative potential (−10V) from the grid of the triode as explained in (2). The anode output circuit becomes high impedance circuit, consisting of the shunt capacitance C_2 and resistance R. The potential drop across the anode circuit load $V(t)$, the voltage observed as the PIC signal, is given in Ref. 1. This signal $V(t)$ is amplified with the 1A4 preamplifier of TEKTRONIX 547 oscilloscope, and smpled at the appropriate time by a linear gate window controlled manually by adjusting the time delay of the slice or automatically by a slew method as shown in Fig. 5.

3. Measurements of Recombiation Coefficients

Plasma is generated in localized columns around the paths of the proton and triton products of the (n,p) reaction in the ^{3}He gas. Hence, the plasma density is not homogeneous over the sensitive volume of the ionization chamber. This inhomogeneous distribution of electrons and ions enhances the average recombination rate over the sensitive volume higher than that for the homogeneous distribution of the same number of electrons

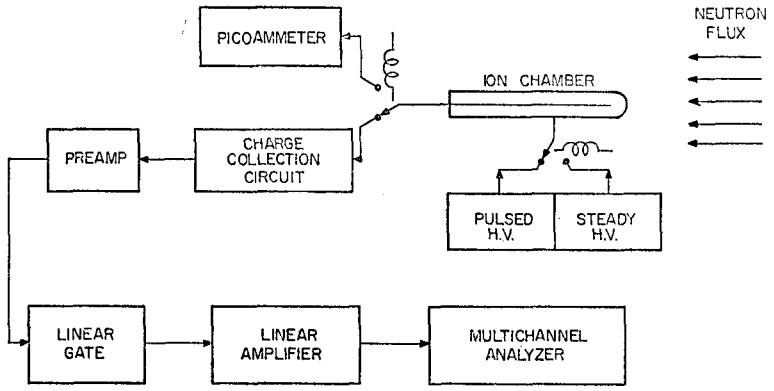

Fig. 6. Simplified version of Fig. 5.

and ions in the same volume, (volume recombinate rate)[2]. The recombination rate observed by the following PIC techniques is the former one.

A) Growth Method.

The general expression for the time rate of change of the electron density N during growth is given Eq. 1. However, this expression can be simplified as the two-body recombination is the predominant loss mechanism for the ^{3}He plasma.[3,4] Hence, the time dependency of the electron density can be written

$$N=\sqrt{S/\alpha_2}[\exp(2\sqrt{S\alpha_2}t)-1]/[\exp(2\sqrt{S\alpha_2}t)+1] \quad (3)$$

by integration when the terms other than S and α_2 are small in Eq. (1).

By measuring the electron densities at the different plasma growth time, t_2-t_1 in Fig. 3, we can trace the time dependency of electron density within the ionization chamber under the constant neutron flux as shown in Fig. 9. Comparison of this measured time dependency of electron density with Eq. (2) can determine the two-body recombination coefficient.

The source term S needed in the measurement can be determined experimentally by measuring the steady state chamber saturation ion current with a constant high voltage potential applied across the chamber electrodes as shown in Fig. 5 and 6. During the measurement, the current is measured with a picoammeter to establish the source ionization rate for each reactor power level for which data is taken. The relationship between the saturated ion current I and the source term S is given by

$$S=I/e\nu \text{ (ion pairs/cm}^3\text{ sec)} \quad (4)$$

where ν is the sensitive volume of the ionization chamber.

B) Steady State Method.

The electron density finally reaches its steady-state asymptotic limit, at which time the generation and the loss by two-body recombination are balanced. Hence, Eq. (2) becomes

$$\alpha_2=S/N^2 \quad (5)$$

at the steady state. Thus, α_2 is determined by N and S at the steady-state measured by the PIC technique and the saturation current measurement in (A), respectively.

4. Experimental Results

In Fig. 7, dots are the signal voltages sliced by a linear gate window at the appropriate time as shown in Fig. 6 for $RC_t \gg \bar{t}_c$ after the

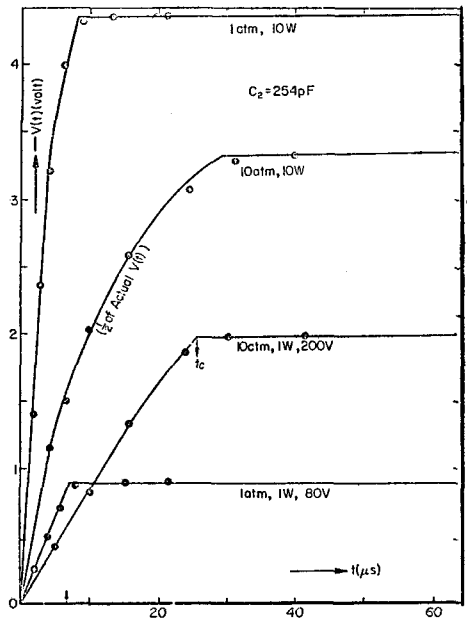

Fig. 7. Signal voltage V *vs* time t from both expeiment and theory.

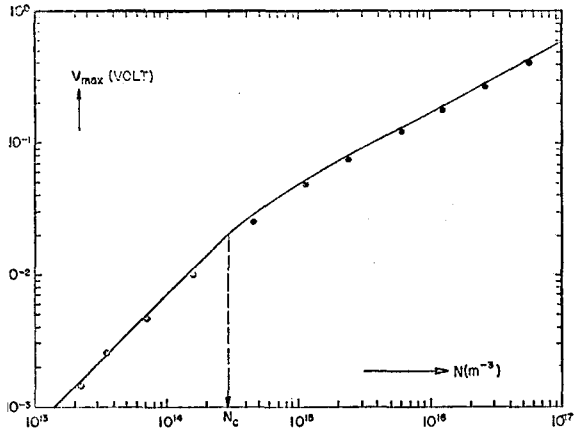

Fig. 8. Maximum signal voltage V_{max} *vs* electron density N from experiment and theory.

electron densities reachs its steady-state asymptotic limit (about 70 ms for t_2-t_1 in Fig. 3) These are compared with theoretical curves based on computer integrations of Eqs. (26) and (27) of Ref. 1. The nuclear reactor power, the collection voltage, and the gas pressure of the chamber are treated as parameters. The nuclear power and the gas pressure of the chamber gives the initial electron density and the mobility, respectively.[5]

In Fig. 8, the maximum signal voltage V_{max} is measured in dependency of the initial electron density N at the steady-state. The electron density of abscissa is calibrated by making use of the following relationships

$$N=\sqrt{S/\alpha^2} \tag{6}$$

from Eq. (5), and

$$N=\frac{C_t V_{max}}{e^{\nu}}\left(1-\frac{1}{2\log(b/a)}\right)^{-1} \tag{7}$$

from Eq. (32) of Ref. 1 for the linear region of V_{max} *vs* $\sqrt{P}$ (P=nuclear reactor power, $P\propto S$) curve. These data are compared with a solid theoretical curve based on a numerical evaluation of Eq. (30) and (31) ($N>Nc$) and Eq. (32) ($N<Nc$), respectively, of Ref. 1.

In Fig. 9, the measured time dependence of electron density during growth is compared with the theoretical curve where the two body recombination is predominant in loss mechanism.

In Fig. 10, the measured two-body recomb-

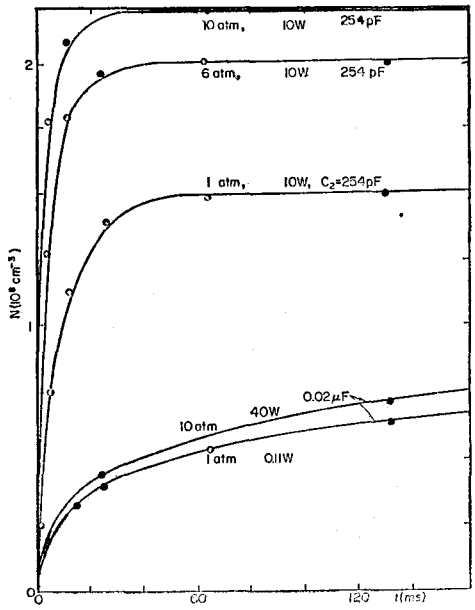

Fig. 9. Time dependence of electron density during growth from both experiment and theory.

ination coefficient by both the growth method and the steady-state method are compared with the theoretical values of Bates and Khare for that of volume recombination.[6]

5. Conclusions

The experimental results of signal voltage are in excellent agreement with the theoretical prediction, showing nonlinear pulse profiles in Fig. 7 and slope change in Fig. 8 for high electron density. Thus, it is possible to apply this technique to measure the electron density of the plasma produced by radiations such as β-ray or γ-ray or by the thermal ionization in high temperature gas. This method has the advantage especially in high pressure gas where the drift velocity of electron is linearly proportional to the electric field, which is the basic condition for the applicability of the theory.

The comparison of the measured time dependence electron density with the theoretical curve shows that the two-body recombination is predominant loss mechanism even for the electron density lower than $10^{14}/m^3$ [7].

The observed two-body recombination rate by the PIC techniques, which is an average of the locally inhomogeneous recombination rate over the sensitive volume of the chamber, is insignificantly different from the theoretical volume recombination rate for the low neutron flux($<10^8/cm^2$-sec) producing plasma in ^3He gas.

Combining the ionization source rate term measured by direct current type operation of the chamber and the electron density obtained from steady-state as well as growth period, the recombination coefficients for electrons were determined as approximately 5×10^{-14}, $3\times10^{-13}(m^3/sec)$ in 1, 10 atmospheric He^3 at room temperature.

References

1. S. H. Kim and W. H. Ellis, J. Appl. Phys. **43**, 3027 (1972)
2. H. E. Wilhelm, J. of Chemical Phys. **47**, 4356 (1967)
3. L. S. Frost and A. V. Phelps, Phys. Rev. **136**, A1538 (1964)
4. L. M. Chanin, A. V. Pheles and M. A. Biondi, Phys. Rev. **128**, 219 (1962).
5. The mobility coefficient k_- is given by
   $k_-=0.83/p$ (m^2/volt-atm)
   where p is the pressure of ^3He gas.
6. D. R. Bates and S. P. Khare, Proc. of Phys. Soc. **85**, 231 (1965).
7. W. H. Ellis, Office of Naval Research, University of Florida, Yearly Summary Technical Report No. 4, 1969 (Armed Service Technical Information Agency Document). In this report, a quite different version of this recombination mechanism is explained by making use of the linear relationship between V_{max} and N for $N>Nc$ under the assumption that space charge effects can be neglected.